Null Synthesis with Phase and Amplitude Controls at the Subarray Outputs

RANDY L. HAUPT, MEMBER, IEEE

Abstract—**The generation of nulls in an antenna pattern by controlling the phase and amplitude of the subarray output signals is investigated. Although the nulls may be formed with any number of subarrays, the subarray configuration and desired null location have a major impact on the distortion in the far-field pattern that results. The distortion problem resulting from subarray nulling is well-known, but little theoretical analysis has been done to explain the cause of the distortion. A theoretical and graphical explanation of why the distortion occurs is offered.**

I. INTRODUCTION

AS THE MICROWAVE spectrum becomes more and more crowded with users, interference rejection techniques become increasingly necessary. One way to reduce the interference is to generate a null in the antenna pattern sidelobes in the direction of the interference. It is possible to form these nulls for a phased array antenna by adjusting the phase and amplitude for the signals received at each element. Large arrays require expensive hardware or a lot of time to form the nulls. In contrast, the nulls can be formed quickly if there are receivers or correlators at every element. Normally, this equipment is not part of the antenna and must be added at considerable cost. On the other hand, forming nulls by "searching" for the best phase and amplitude settings avoids the expensive equipment, but takes considerable time to form the nulls.

One way to reduce either the amount of extra hardware or the time to form the null is to control the signal characteristics at the subarray output rather than at the individual element outputs [1], [2]. Often a large array is divided into subarrays in order to place time delay units at the subarray outputs. Arrays sometimes need time delay units to receive wide bandwidth signals properly. Time delay units are very expensive and bulky so they are usually not placed at every element in the array. Thus, only the subarray outputs receive a true time delay. Subarray outputs also offer convenient locations to put controls that modify the signals to generate nulls in the far-field pattern. Fewer signals to control implies either less hardware or less time needed to form nulls. These advantages make subarray nulling very attractive.

The problem of antenna pattern distortion due to subarray nulling is well-known. Reducing the number of signal controls in the array in turn reduces the amount control over the far-field pattern. This paper illustrates why that distortion occurs.

II. NULL SYNTHESIS

This section explores the limitations to forming nulls with phase and amplitude controls at the subarray outputs. Fig. 1 is a linear array divided into M contiguous subarrays of N elements per subarray. Each array element has a beam-steering phase shifter. For the purpose of this analysis, the phase shifters are assumed to be set for maximum gain at boresite. The amplitude weights correspond to an amplitude taper, such as a Taylor distribution. In addition, a phase shifter and time delay unit appear at the output of each subarray. Since the main beam is assumed to be at boresite, then all the time delay units are set at zero and can be ignored in the analysis.

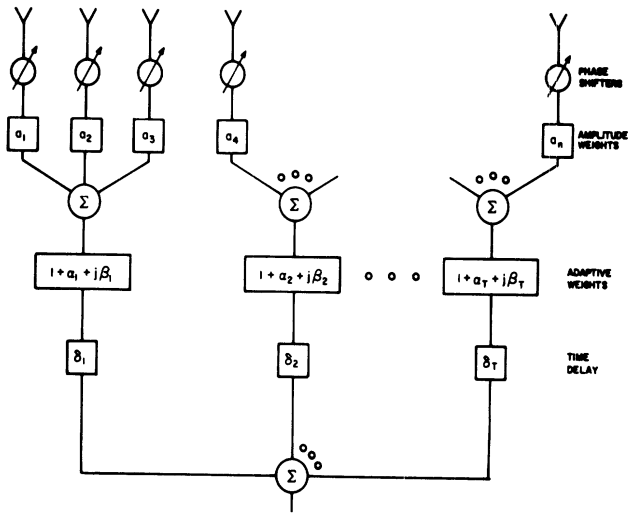

Fig. 1. Linear array divided into subarrays.

Equation (1) gives the far-field pattern of a linear array of M subarrays and N elements per subarray.

$$F(u) = \sum_{m=1}^{M} (1 + \alpha_m + j\beta_m) \sum_{n=1}^{N} a_{mn} \exp(jkd_{mn}u) \tag{1}$$

where

$1 + \alpha_m + j\beta_m$	adjustable complex weight at subarray m
a_{mn}	amplitude weight at element n of subarray m
k	wavenumber $= 2\pi/\lambda$
λ	wavelength
d_{mn}	distance in λ from center of array to element n in subarray m
u	$\sin\theta$
θ	direction from boresite.

Ideally, the antenna forms a null in the direction of interference. In other words $F(u_q) = 0$ when u_q is in the direction of an interference source and $q = 1, 2, \cdots, Q$. The nulls appear in the desired direction when the complex weights at the subarray outputs (written here in real and imaginary form) are set at the proper values.

If nulls form in Q desired directions then [3]

$$\sum_{m=1}^{M} (1 + \alpha_m + j\beta_m) \sum_{n=1}^{N} a_{mn} \exp(jkd_{mn}u_d) = 0, \quad q = 1, 2, \cdots, Q \tag{2}$$

$$\sum_{m=1}^{M} \sum_{n=1}^{N} a_{mn} \exp(jkd_{mn}u_q) + \sum_{m=1}^{M} (\alpha_m + j\beta_m) \sum_{n=1}^{N} a_{mn} \cdot \exp(jkd_{mn}u_q) = 0 \tag{3}$$

Manuscript received May 21, 1984; revised December 10, 1984.
The author was with the Electromagnetic Sciences Division, Rome Air Development Center, Hanscom AFB, MA. He is now with the Radiation Laboratory, University of Michigan, Ann Arbor, MI 48109.

$$\sum_{m=1}^{M}(\alpha_m + j\beta_m)\sum_{n=1}^{N} a_{mn}\exp(jkd_{mn}u_q)$$

$$= -\sum_{m=1}^{M}\sum_{n=1}^{N} a_{mn}\exp(jkd_{mn}u_q). \quad (4)$$

Equation (4) represents a set of equations with M unknowns. Consequently, the equation may be written in the matrix form $\mathbf{AX} = \mathbf{B}$ where

$$\mathbf{A} = \begin{bmatrix} \sum_{n=1}^{N} a_{1n}\exp(jkd_{1n}u_1) & \cdots & \sum_{n=1}^{N} a_{Mn}\exp(jkd_{Mn}u_1) \\ \vdots & & \vdots \\ \sum_{n=1}^{N} a_{1n}\exp(jkd_{1n}u_Q) & & \sum_{n=1}^{N} a_{Mn}\exp(jkd_{Mn}u_Q) \end{bmatrix}$$

$$\mathbf{X} = \begin{bmatrix} \alpha_1 + j\beta_1 \\ \vdots \\ \alpha_m + j\beta_m \end{bmatrix}$$

$$\mathbf{B} = \begin{bmatrix} -\sum_{m=1}^{M}\sum_{n=1}^{N} a_{mn}\exp(jkd_{mn}u_1) \\ \vdots \\ -\sum_{m=1}^{M}\sum_{n=1}^{N} a_{mn}\exp(jkd_{mn}u_Q) \end{bmatrix}.$$

$\mathbf{X}$ has a unique solution when $Q = M$. Usually, though, $Q < M$ and several different values of $\mathbf{X}$ satisfy the equation $\mathbf{AX} = \mathbf{B}$. Small values for the complex weights will disturb the far-field pattern less than larger values. Thus, of the many possible values for $\mathbf{X}$, the best results occur from minimizing $\Sigma(\alpha^2 + \beta^2)$. Solving $\mathbf{AB} = \mathbf{B}$ while minimizing the complex weights gives [4]

$$\mathbf{X} = \mathbf{A}^{\dagger}(\mathbf{A}\mathbf{A}^{\dagger})^{-1} \quad (5)$$

where $\mathbf{A}^{\dagger}$ is the transpose conjugate of matrix $\mathbf{A}$. Solving (4) in matrix form gives the following values for the elements in the complex matrix $\mathbf{X}$:

$$\alpha_m = \sum_{q=1}^{Q}\sum_{n=1}^{N} a_{mn}[Y_q\cos(kd_{mn}u_q) + Z_q\sin(kd_{mn}u_q)] \quad (6)$$

$$\beta_m = \sum_{q=1}^{Q}\sum_{n=1}^{N} a_{mn}[Z_q\cos(kd_{mn}u_q) - Y_q\sin(kd_{mn}u_q)]. \quad (7)$$

The variables Y_q and Z_q are elements of a complex array W given by

$$\mathbf{W} = (\mathbf{A}\mathbf{A}^{\dagger})^{-1}\mathbf{B}. \quad (8)$$

Fig. 2 shows the quiescent far-field pattern of a 24-element array of isotropic sources spaced 0.5 λ apart and having a uniform amplitude distribution. Figs. 3(a) and 4(a) show the results of nulling with an interference source at 8° and with eight and four subarrays, respectively. As the number of subarrays decrease, the distortion to the antenna pattern increases. The increase in distortion is not significant, though.

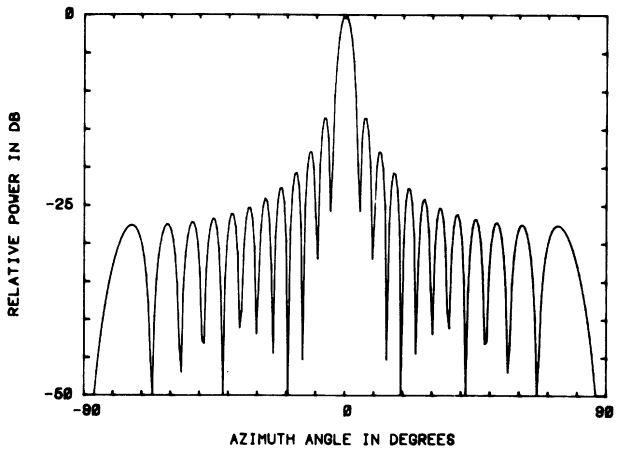

Fig. 2. Quiescent far-field pattern of a 24-element uniform array.

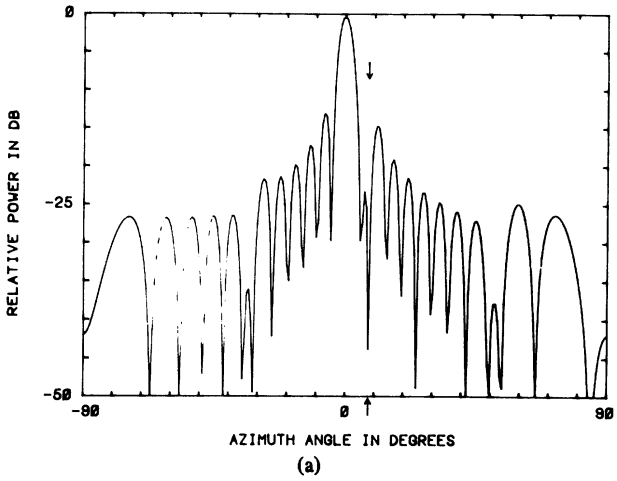

Fig. 3. Placing a null at 8° with eight subarrays. (a) Far-field pattern. (b) Cancellation beam superimposed on quiescent pattern.

Problems with pattern distortion occur when the null is formed outside of the subarray pattern. A subarray pattern is the far-field pattern of an individual subarray with its peak centered at 0°. Although the amplitude tapers for each subarray are different, their beamwidths are about equal because they are all the same size. The null-to-null beamwidth BW of a uniformly illuminated array with N elements spaced 0.5 λ apart is given by

$$\mathrm{BW} = 2\sin^{-1}(2/N). \quad (9)$$

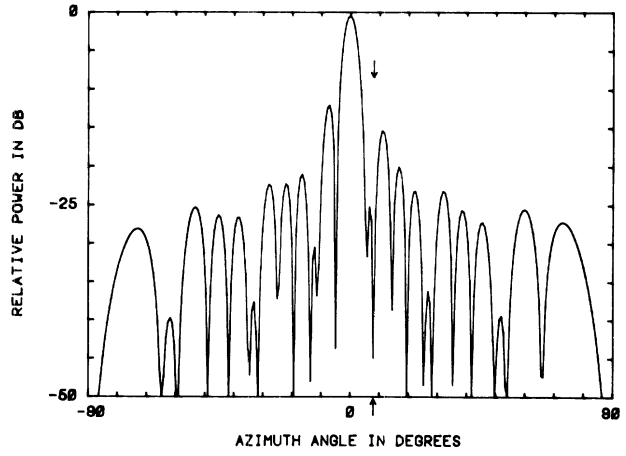

(a)

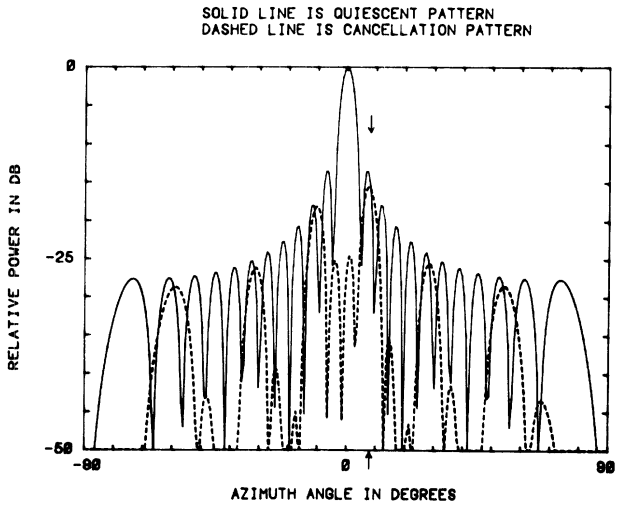

(b)

Fig. 4. Placing a null at 8° with four subarrays. (a) Far-field pattern. (b) Cancellation beam superimposed on quiescent pattern.

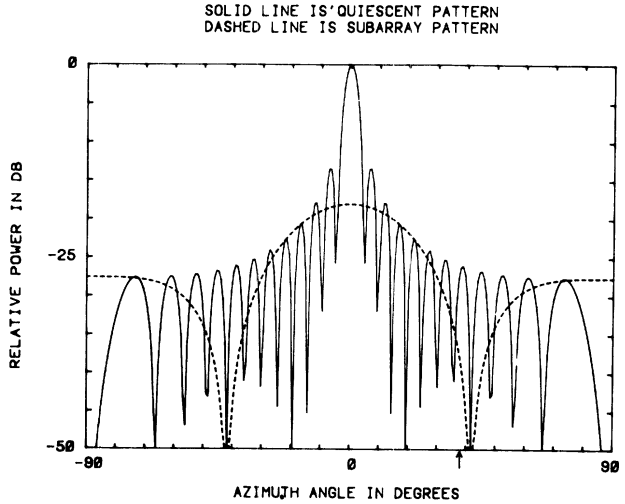

Fig. 5. Far-field pattern of a three-element subarray superimposed on the quiescent pattern.

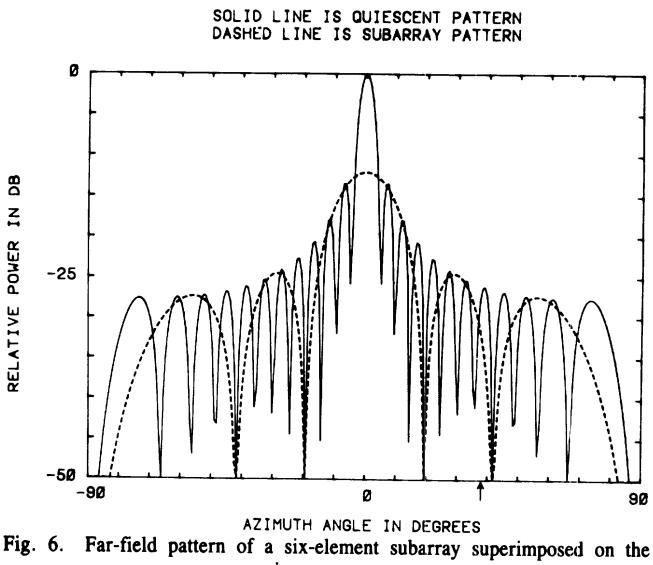

Fig. 6. Far-field pattern of a six-element subarray superimposed on the quiescent pattern.

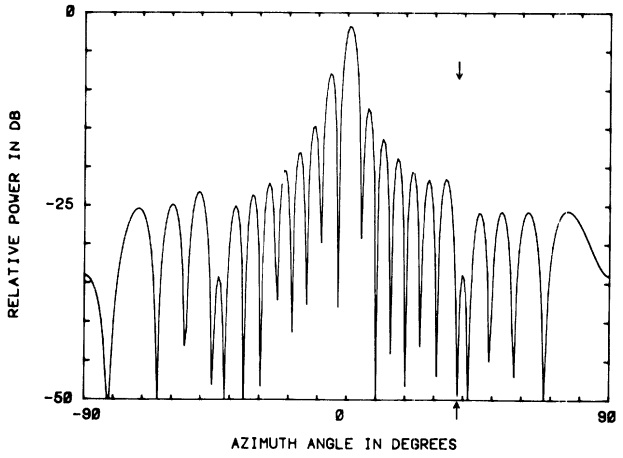

(a)

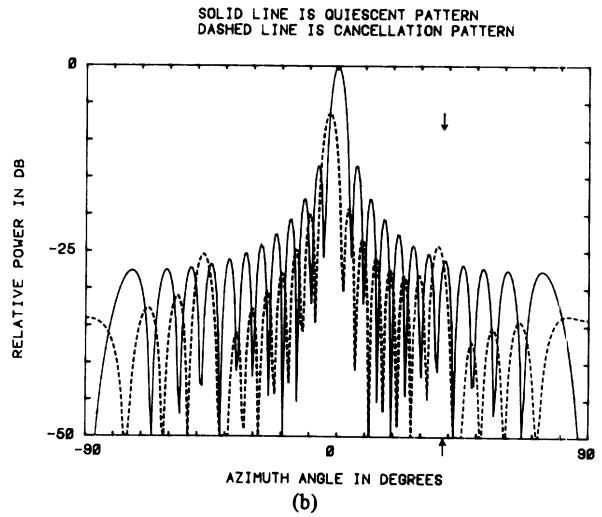

(b)

Fig. 7. Placing a null at 38° with eight subarrays. (a) Far-field pattern. (b) Cancellation beam superimposed on quiescent pattern.

The null-to-null beamwidths for three and six elements are 84° and 39°, respectively. An isotropic element has no null-to-null beamwidth because it radiates equally in all directions. Figs. 5 and 6 show the subarray patterns superimposed on the quiescent pattern for $N = 1$, 3, and 6 elements. If our initial premise of nulling inside the subarray pattern produces less distortion than nulling outside the subarray pattern is true, then an interference source at 38° should produce more distortion than one at 8°. The distortion should not change for the 24-subarray case because the subarray pattern is isotropic (see Fig. 6). However, the eight and four subarray cases should show a marked degradation.

Figs. 7(a) and 8(a) are the resulting patterns after placing a null at 38°. As predicted, when there were 24 subarrays, the amount of distortion did not change when the interference loca-

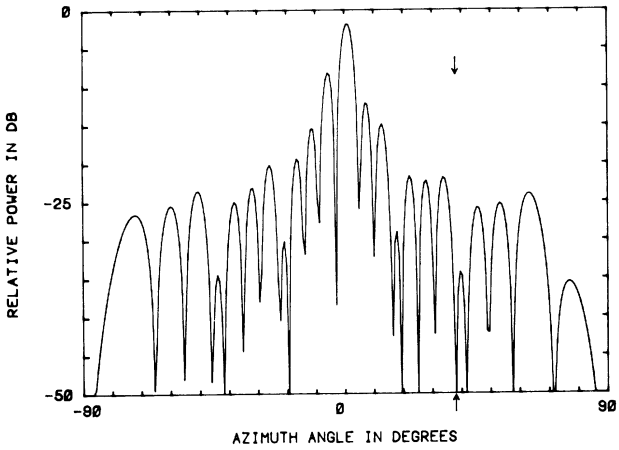

(a)

SOLID LINE IS QUIESCENT PATTERN
DASHED LINE IS CANCELLATION PATTERN

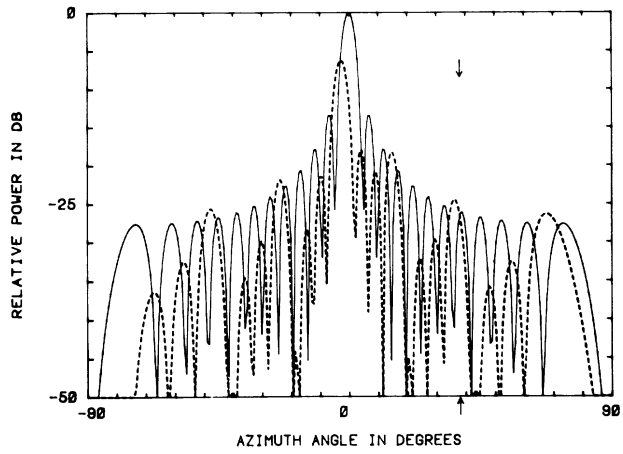

(b)

Fig. 8. Placing a null at 38° with four subarrays. (a) Far-field pattern. (b) Cancellation beam superimposed on quiescent pattern.

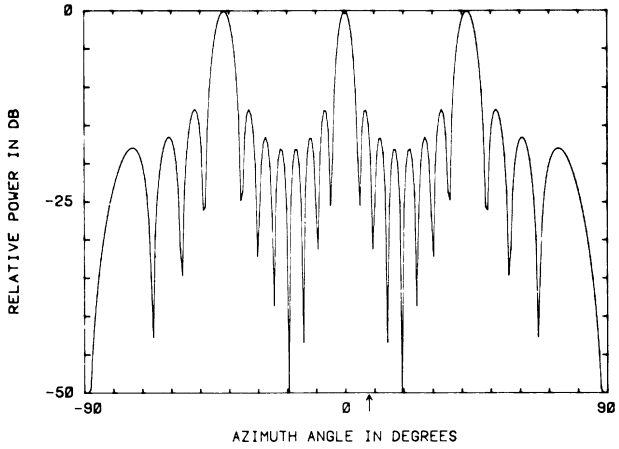

Fig. 9. Array factor for an eight-element array with a spacing of 1.5 λ.

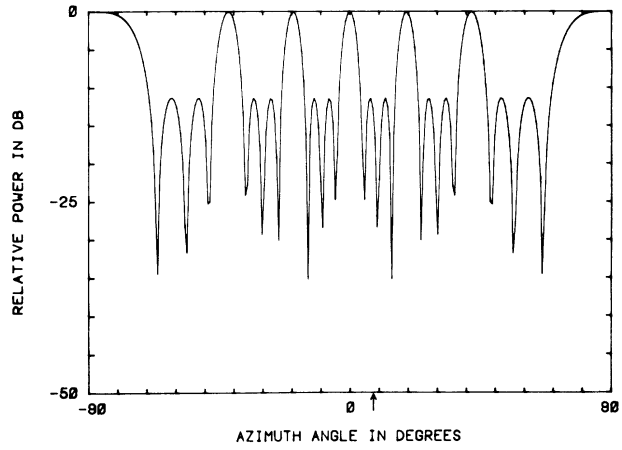

Fig. 10. Array factor for a six-element array with a spacing of 3.0 λ.

tion moved. Because the interference location moved outside or nearly outside the subarray pattern, the amount of distortion to the far-field pattern increased substantially. The next section offers an explanation of this distortion phenomenon.

III. CAUSES OF FAR-FIELD PATTERN DISTORTION

Far-field pattern distortion caused by subarray nulling limits its use. The limitations are fundamental and do not depend on the technique that generates the nulls. This limitation is best illustrated by examining the cancellation beam that adds to the quiescent pattern to form the null. Equation (3) is written in the form

$$\text{quiescent pattern} + \text{cancellation pattern} = 0$$

at the desired null location. The nulling technique forms a cancellation pattern that has the same amplitude, but is 180° out of phase with the quiescent pattern at the interference location. Adding the two patterns together produces a null in the direction of the interference.

The cancellation beams that produce the adapted patterns in part (a) of Figs. 3, 4, 7, and 8 are shown in part (b) of those same figures. When the array is fully adaptive (24 subarrays), the cancellation beam has one peak and no grating lobes. Grating lobes do not enter real space in the array factor because the elements are space 0.5 λ apart. Since the element pattern is isotropic, the cancellation pattern and array factor are identical.

When the array is divided into subarrays, it may be considered as an array of M elements spaced $N\lambda/2$ apart. Each array element, or subarray, now consists of N isotropic antennas. The subarray patterns appear in Figs. 5 and 6. Adjusting the phase and amplitude of the signals at the subarray outputs does not change the subarray patterns, however, controlling the subarray output signals can modify the array factor. Figs. 9 and 10 show the quiescent array factors for $M = 8$ and 4, respectively. The array factors have grating lobes because of the large element (subarray) spacing. Grating lobes appear at predictable locations given by the formula

$$\theta = \pm\sin^{-1}\,[x/Nd] \tag{10}$$

where $x = 1, 2, 3$ and d = element spacing.

The problem of pattern distortion associated with subarray nulling is due to the grating lobes in the array factor. As the array factor beam moves away from boresite, the product of this beam and the subarray pattern decreases. In addition, the first grating lobe begins to move inside the subarray beam. Consequently, the peak of the cancellation beam decreases in size while the grating lobe becomes larger in size. Adding the cancellation pattern to the quiescent pattern creates a null in the specified direction, but causes distortion to the pattern in the direction of the grating lobe.

Consider what happens when a null is placed in the antenna pattern with eight subarrays. The three-element subarray pattern is shown in Fig. 5. From the above discussion, one would expect little distortion to the antenna pattern where nulling at the peak of a sidelobe between 0° and 15°, because the grating lobe of

TABLE I
COMPARISON OF THE RELATIVE POWER LEVEL OF THE CANCELLATION PATTERNS AND SUBARRAY PATTERNS

Null Location	Number of Subarrays	Mainbeam and Grating Lobe Locations	Relative Levels* of Cancellation Pattern	Relative Levels* of Subarray Pattern	Associated Figures
8°	8	8°	-15.6 dB	-18.6 dB	3, 5, 9
		33.8°	-28.4	-31.4	
21°	8	21°	-24	-22.2	
		20.8°	-23.9	-22.1	
38°	8	38°	-26.5	-38.4	5, 7, 9
		-3.8°	-46.3	-18.2	
8°	4	8°	-15.6	-14.6	4, 6, 10
		-11.5°	-18.8	-17.8	
		-33.8°	-27.6	-26.6	
21°	4	21°	-24	-34.8	
		1.5°	-1.3	-12.1	
		-20.8°	-25.1	-35.9	
38°	4	38°	-26.5	-32.6	6, 8, 10
		18.5°	-31.5	-37.6	
		-3.8°	-6.5	-12.6	

* in dB relative to the peak gain of a uniform array of 24 elements

the cancellation pattern is smaller amplitude in than the mainbeam of this pattern. Between 15° and 30°, the grating lobe grows and gradually becomes larger than the main beam. From 30° to 40° the grating lobe is significantly greater than the main beam of the cancellation pattern.

Figs. 3(a) and 3(b) show the results of placing a null at 8°, and Figs. 7(a) and 7(b) result from a null at 38°. Note how the cancellation beam grows smaller as the grating lobe grows larger when the null moves further away from boresite. This increase in grating lobe amplitude corresponds to the increase in distortion to the nulled pattern.

A similar analysis is possible with the four subarray example, except the amount and location of the distortion changes. Since the subarray pattern (Fig. 5) has a much narrower main beam, distortion becomes more of a problem as the null moves away from boresite. This fact is evident in Figs. 4(a) and 8(a). The corresponding (b) parts of these figures show the change in the cancellation beam and grating lobe.

The amount of distortion to the antenna pattern may be estimated from the location of the grating lobes, the subarray pattern, and the height of the quiescent sidelobe before nulling. Below is a list of the grating lobe locations for the eight-element array factor and four element array factor. These were calculated from (10) and can be seen in Figs. 9 and 10.

eight elements ±41.8°
four elements ±19.5°, ±41.8°, ±90°.

The relative levels of the subarray pattern at the array factor main beam location and some grating lobe locations are given in Table I. Also the relative levels of the cancellation beam at these locations are given. The subarray pattern and the cancellation beam have the same relative difference between them at the locations listed. This proportional difference results from the product of the array factor and the subarray pattern that leads to the cancellation beam.

The relative levels of the subarray pattern and cancellation pattern at the array factor main beam and grating lobe locations gives an idea of how much the antenna pattern will be distorted due to nulling. Look at the figures associated with the entries in Table I and see how the far-field pattern distortion relates to the subarray pattern. The lower the level of the subarray pattern in the direction of the desired null, the greater the pattern distortion becomes when the null is formed.

A conservative estimate of the angular limit of subarray nulling is given in (11):

$$\theta_{\text{null}} = \pm 0.5 \sin^{-1} [1/(Nd)]. \tag{11}$$

at $\pm\theta_{\text{null}}$ the peak of the cancellation beam is the same height as one of the first grating lobes. Beyond this angle the grating lobe gain becomes larger than that of the main beam.

One final point worth mentioning is that the distortion would be greater in the neighborhood of a null in the subarray pattern. The amount of distortion would improve when the null was placed in the same location as the peak of a subarray pattern sidelobe. For instance, a null placed at 38° with eight subarrays produces considerably more distortion then a null placed at 60°. The null at 38° is close to the null in the subarray while 60° is almost at the peak of the subarray pattern sidelobe.

IV. CONCLUSION

This paper illustrates theoretically the pattern distortion problem associated with subarray nulling. The amount of distortion to the far-field antenna pattern is inversely proportional to the subarray far-field pattern. Thus, subarray nulling near the mainbeam produces little distortion. On the other hand, the distortion increases dramatically when the null is placed further from the main beam.

REFERENCES

[1] D. J. Chapman, "Partial adaptivity for the large array," *IEEE Trans. Antennas Propagat.*, vol. AP-24, pp. 685-696, Sept. 1976.
[2] D. R. Morgan, "Partially adaptive array techniques," *IEEE Trans. Antennas Propagat.*, vol. AP-26, pp. 823-833, Nov. 1978.
[3] R. L. Haupt, "Nulling with limited degrees of freedom," RADC-TR-83-114, Apr. 1983.
[4] R. A. Shore and H. Steyskal, "Nulling in linear array patterns with minimization of weight perturbations," RADC-TR-82-32, Feb. 1982.

Randy L. Haupt (M'82), for a photograph and biography please see page 493 of the May 1984 issue of this TRANSACTIONS.